JOURNAL OF CATALYSIS **124,** 416–432 (1990)

Morphology and Activity of MoS_2 on Various Supports: Genesis of the Active Phase

KERRY C. PRATT, JOHN V. SANDERS, AND VICTOR CHRISTOV

CSIRO Division of Materials Science and Technology, Locked Bag 33, Clayton, Victoria, Australia 3168

Received March 13, 1989; revised February 12, 1990

The morphology and hydrodesulfurization (of thiophene) activity of unpromoted MoS_2 supported on alumina, silica, titania, and zirconia have been examined. In the oxidic catalyst, no surface molybdenum phases could be identified by transmission electron microscopy. For all supports except titania, an additional bulk molybdenum oxide phase appeared above a particular Mo loading. In the case of the alumina support, bulk $Al_2(MoO_4)_3$ also appeared. In the sulfided catalysts, the bulk species retained their original morphology and were surrounded by a skin of MoS_2 several layers thick. The core of the bulk MoO_3 was reduced to Mo metal. On the surface of the SiO_2 and Al_2O_3, the MoS_2 was present as flakes up to five layers thick, sitting vertically on the support. For TiO_2 and ZrO_2 the MoS_2 was present as "islands," which expanded with increased Mo loading, eventually encapsulating the support particles. The reactivity behavior also fell into two groups, corresponding to the two forms of MoS_2 morphology. The specific activity of MoS_2 supported on TiO_2 and ZrO_2 was higher than that for the case of Al_2O_3 and SiO_2 supports.

INTRODUCTION

Catalysts based on Mo (or W) and promoted by Ni or Co are widely used in the petroleum industry for the hydrodesulfurization (HDS) of petroleum feedstocks (*1*). Interest in these catalyst systems has recently been heightened by the perceived need for large-scale processing of liquids derived from coal or oil-shale at some time in the future. However, in spite of their wide and longstanding use, a complete explanation of the nature of the active sites and their mode of action still awaits formulation.

Because of the reaction environment, the operational forms of these catalysts are like those of their sulfides. It is generally accepted that MoS_2 (or WS_2) is the catalyst, with reactive sites modified in some way by the promoter atoms (Ni or Co). In the past decade, three models describing the action of the promoter in sulfided catalysts have emerged as deserving serious attention. These are, first, the intercalation model (*2*) in which it is proposed that the Co (or Ni) is intercalated into octahedral sites at the edges between the MoS_2 (or WS_2) slabs (i.e., between adjacent sulfur layers). Second, the contact synergy model (3–5) of Delmon in which it is proposed that the Group VIII metal sulfide exists as a separate phase (NiS_2 or Co_9S_8) from which spill-over of hydrogen to the MoS_2 phase can occur. Finally, Topsøe and co-workers (*6, 7*) have proposed the existence of the so-called "Co-Mo-S" phase as the predominant active species in promoted catalysts. While this model is similar in some respects to the intercalation model, in the Co-Mo-S phase, the Co (or Ni) is thought to be located in the same plane as that of the Mo atoms, possibly in interstitial or substitutional positions.

Although recent experimental evidence (*8, 9*) suggests that the promoter atoms are indeed located at the edges of the MoS_2 sheets, high-resolution electron microscopy studies (*10, 11*) show that the predominant morphology of MoS_2 in operating catalysts is as single sheets. It seems unlikely therefore that promoter intercalated between MoS_2 sheets is important.

It has been observed that the support has

0021-9517/90 $3.00

a marked effect on the activity of sulfide catalysts (e.g., Refs. (*12–15*)), and this has been attributed to the ability of the support to stabilize MoS_2 at high dispersion (*6, 12*). Of the models above, only the Co-Mo-S model directly attributes a role to the support. It has been suggested that MoS_2 may be regarded as the "primary" support, with alumina, carbon, etc., acting as a "secondary" support (*7*) which allows stabilization of highly dispersed MoS_2 structures capable of accommodating large amounts of promoter atoms around the edges. Such a role may also be ascribed to the support in connection with the "contact synergy" model.

It appears likely then that the first requirement of an active catalyst is for the generation and stabilization of highly dispersed MoS_2, which is then modified in some way by the promoter atoms. The genesis of the MoS_2 on the support is therefore of vital importance. In order to understand this process, it is useful to observe the nature of the oxidic precursors and the process of their transformation to the sulfide form.

We have used transmission electron microscopy (TEM) to study the structural and morphological changes accompanying the process for unsupported Ni-Mo catalysts (*16, 17*). In this paper, we extend our studies to supported catalysts, using a range of support materials. In this first instance, the study is limited to unpromoted molybdenum catalysts.

EXPERIMENTAL

(*i*) *Catalyst Preparation*

Unpromoted molybdenum catalysts containing varying amounts of Mo were prepared on commercial support materials consisting of γ-alumina, silica, titania (anatase), and zirconia. Catalysts were manufactured by the method of incipient wetness. The appropriate amount of $(NH_4)_6Mo_7O_{24} \cdot 4H_2O$ was dissolved in sufficient distilled water to cause incipient wetness. This was added to 2 g of support (60–80 mesh), heated at 353 K for 2 h, and then allowed to evaporate to dryness. A further quantity of distilled water (incipient wetness) was added, and again evaporated to dryness. This procedure was repeated once more. The catalyst was then dried overnight at 393 K and subsequently calcined in air for 4 h at 673 K.

(*ii*) *Catalytic Activity*

The fixed-bed microreactor and the chromatographic analysis employed in these studies were essentially the same as those described earlier (*16*).

A catalyst charge of about 0.5 g, together with an equal volume of glass beads (of the same size range) was employed. The catalysts were sulfided by a stream of 20% v/v H_2S/H_2 at 673 K for 2 h. Hydrogen saturated with thiophene in a bubbler maintained at 273 K was then passed over the catalyst until product analysis indicated a steady-state (usually 3–4 h). All runs were carried out at 648 K. Activity was expressed as a pseudo-first-order rate constant.

(*iii*) *Transmission Electron Microscopy*

Catalyst samples (without glass beads) were subjected to sulfiding and reaction as above. The reactor was then cooled under a nitrogen flow, and the catalyst removed and stored under a nitrogen blanket. Samples were prepared by ultrasonic dispersion in ethyl alcohol, and a portion was collected on a holey carbon film mounted on a specimen grid. They were examined in a JEOL 100 CX top entry electron microscope, fitted with an objective lens for which $C_s = 0.7$ mm.

RESULTS

(*i*) *Activity Studies*

The composition data and the activities of the catalyst are shown in Table 1. These data appear to demonstrate an optimum molybdenum content for each catalyst. This behavior is similar to other results in the literature (e.g., Ref. (*19*)). The magnitudes of the activities are largely a reflection of the differing support surface area in this raw (uncorrected form).

TABLE 1

Catalyst Characteristics and Activity for HDS of Thiophene Expressed by Pseudo-First Order Rate Constants at 648 K

Catalyst	% MoO_3	at. Mo nm^{-2}	k ($\times 10^2$) ($cm^3\ s^{-1}\ g^{-1}$)	k (at. Mo)$^{-1}$ ($\times 10^{21}$)
Al_2O_3	0	—	—	—
	2	0.3	20	2.39
Surface	5	0.75	61	2.92
area =	10	1.50	130	3.10
240 $m^2\ g^{-1}$	15	2.25	155	2.47
	20	3.0	170	2.03
	30	4.5	140	1.15
	40	6.0	120	0.72
SiO_2	0	—	—	—
	5	0.59	56.8	2.72
Surface	10	1.20	138.8	3.32
area =	15	1.80	161.2	2.56
350 $m^2\ g^{-1}$	20	2.40	179.0	2.14
	30	3.60	225.6	1.80
	40	4.80	192.4	1.14
TiO_2	0	—	—	—
Surface	1	0.97	22.0	5.26
area =	3	2.91	52.0	4.14
43 $m^2\ g^{-1}$	6	5.84	65.0	2.59
	10	9.73	46.0	1.09
ZrO_2	0	—	—	—
	1	2.33	15.0	3.58
Surface	3	6.97	26.0	2.07
area =	6	13.98	27.0	1.08
18 $m^2\ g^{-1}$				
	10	23.30	21.5	0.51

(ii) Electron Microscopy Studies

Figure 1 shows transmission electron micrographs of the untreated support materials.

(a) The Oxide Phases

At all concentrations of Mo, the surfaces of the support materials were in appearance similar to the untreated support. In particular, no surface phases of molybdenum oxide could be discerned. While there appeared to be some decrease in definition at the edge of the particles, there was no evidence of patchiness on the surface. Even careful examination of a through-focus series of Mo-γ-Al_2O_3 revealed nothing, whereas it had been thought that some decoration of steps might be observed.

At higher concentrations of Mo, a separate phase consisting of angular crystals (approximately 1 μm square) appeared and was identified by electron diffraction as MoO_3. An example of these crystals for the case of the zirconia support is shown in Fig. 2. The lowest concentration of Mo at which these oxide crystals were detected on the various supports is listed in Table 2. This was determined visually by scanning an area of about 1 grid at a relatively low magnification (10,000×). As seen from Table 2 the additional phase of MoO_3 was detected on all supports, except TiO_2. Leyrer *et al.* (*20*) also found no formation of bulk MoO_3 on TiO_2 supports.

For the alumina-supported systems containing 10% w/w MoO_3 or more, a second bulk phase was observed. This consisted of rounded crystals, about 20 nm in size, linked into short chains and forming open tubular clusters several micrometers in size. These are shown in Fig. 3a. Electron diffraction patterns contained spacings consistent with those of $Al_2(MoO_4)_3$ (ASTM 23-764), but with some additional spacings. No evidence for lines from $Al_2(MoO_4)_3$ was found in the XRD traces, and observed reflections fitted the pattern expected from MoO_3. No similar structures were observed on the other supports.

(b) The Sulfide Phases

XRD traces displayed no evidence of any crystalline material. Below we describe TEM observations on the various components of the sulfided catalysts.

(i) The bulk phases. In those catalysts

TABLE 2

Concentrations of MoO_3 at Which Bulk Crystals of MoO_3 Are First Detected in Electron Micrographs

Catalyst support	Loading (% w/w)
γ-Al_2O_3	15
SiO_2	10
ZrO_2	3
TiO_2	—

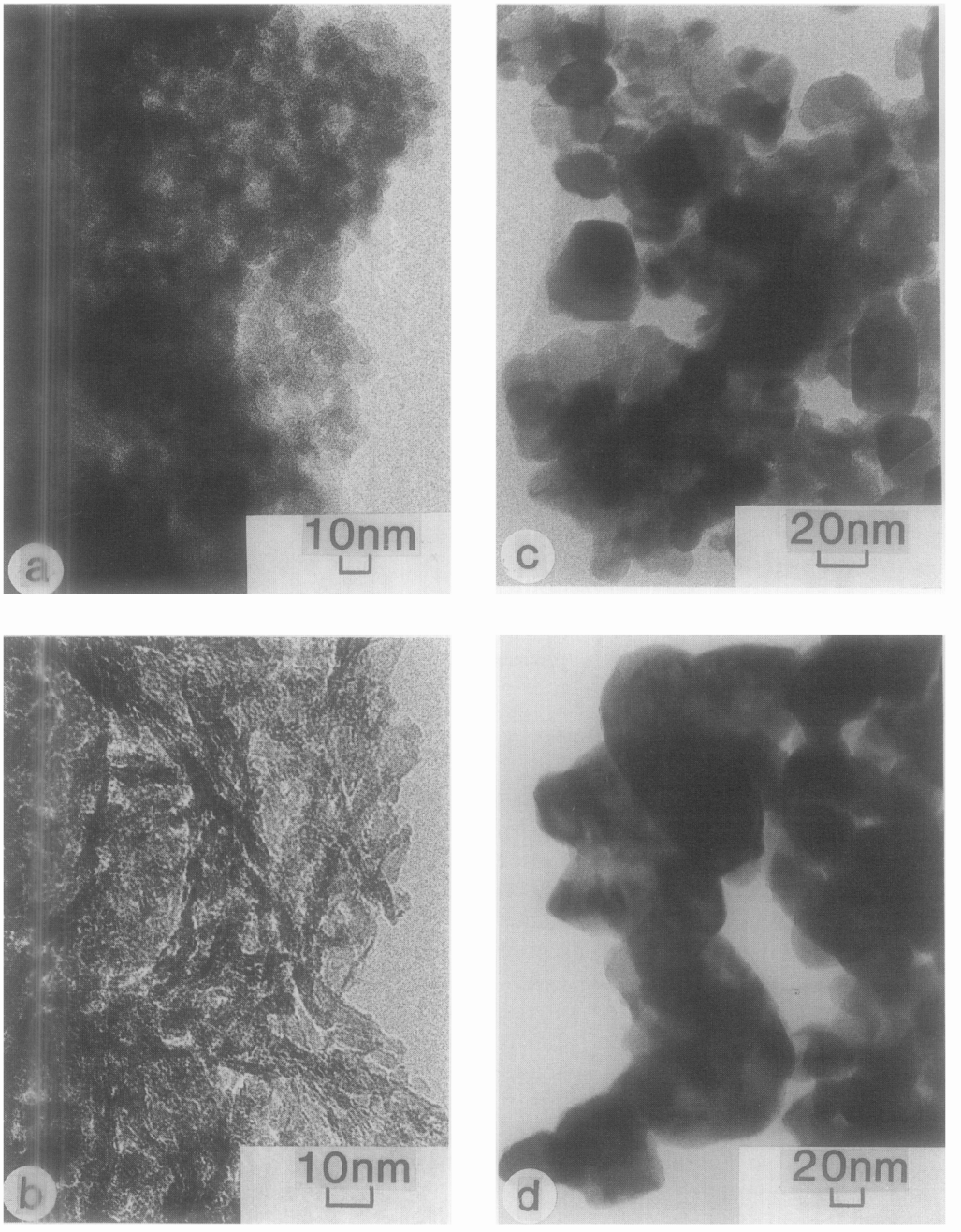

FIG. 1. Transmission electron micrographs of the support materials used in the experiments: (a) SiO_2; (b) γ-Al_2O_3; (c) TiO_2 (anatase); (d) ZrO_2.

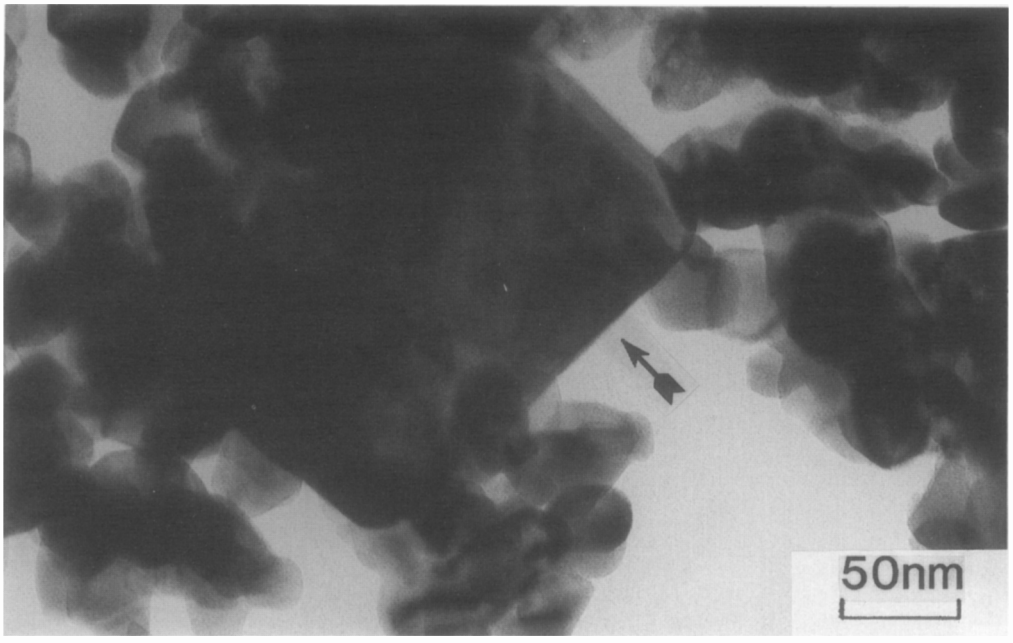

FIG. 2. Electron micrograph of MoO_3 on zirconia. Where ZrO_2 is impregnated with more than about 5% w/w MoO_3, bulk crystals of MoO_3 (identified by electron diffraction) can be distinguished by their square or rectangular shape (arrowed).

where there was originally MoO_3 present as a separate phase, it was still recognizable by its morphology at low magnifications after sulfidation. At higher magnifications (Fig. 4) the crystals were found to expose a surface skin, about 5–10 layers thick, of disordered MoS_2 which appeared in the images as sets of fringes, roughly parallel to the surface of the crystal. Electron diffraction patterns gave rings consistent with the 001 spacings of MoS_2 and sets of diffuse spots. The insert of Fig. 4 shows such a pattern from a crystal intentionally tilted so that the electron beam is parallel to a zone axis. This pattern of diffuse spots corresponds to a *bcc* structure with a lattice parameter of 0.572 nm, which is only slightly different from that expected for molybdenum. The image of the interior of the crystal appeared speckled. We deduce therefore that the MoO_3 crystals have been converted to sulfide only on the surface, and that the interior has been reduced to Mo, in a highly disordered form, or as a collection of very small crystals in approximately the same orientation. This observation was common to all those samples containing excess Mo in the form of MoO_3 crystals as a separate phase.

The $Al_2(MoO_4)_3$ chain structures sulfided to produce a material skinned by two to three layers of MoS_2 over a disordered material giving no regular lattice images and only very diffuse scattering (see Fig. 3b). The electron diffraction pattern contains sharp (100) and (110), but no (001) or (*hkl*) reflections from MoS_2.

The structure and morphology of the MoS_2 present as a surface phase was different on the various supports and will be described individually.

(*ii*) *Surface sulfide phase on* γ-Al_2O_3. In accordance with previous observations (*19*), the MoS_2 was highly dispersed, generally as individual S-Mo-S sheets about 2–10 nm in size. (The size was estimated by measuring the length of sheets in the electron

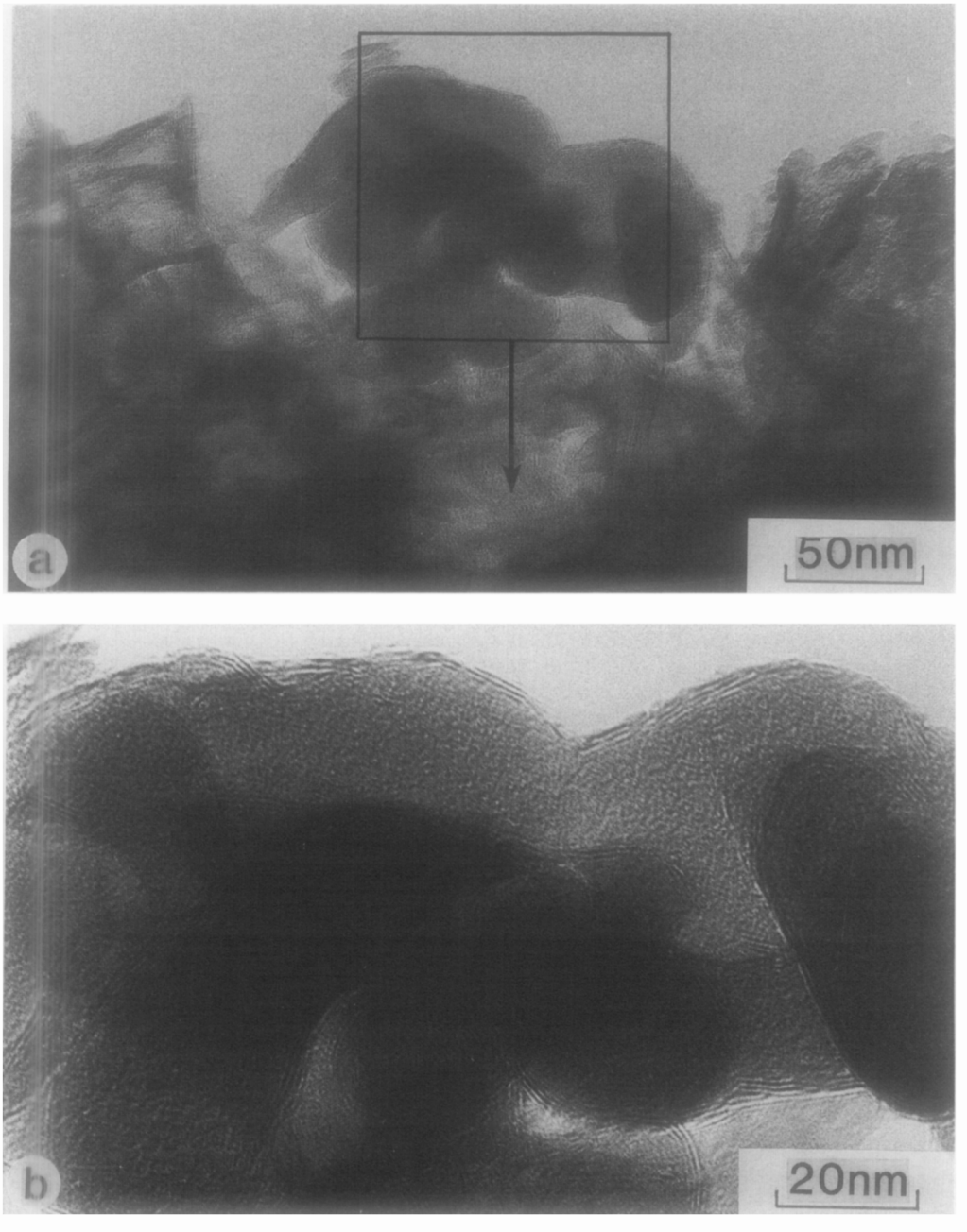

FIG. 3. Electron micrographs of the bulk "tubular" phase which appeared with >10% w/w MoO_3 on γ-Al_2O_3. The appearance at low magnification (a) is similar in calcined and sulfided catalysts. However, after sulfiding, at high magnification (b), the surface is found to be coated with a layer of MoS_2, about three sheets thick. (Twenty percent MoO_3 on alumina.)

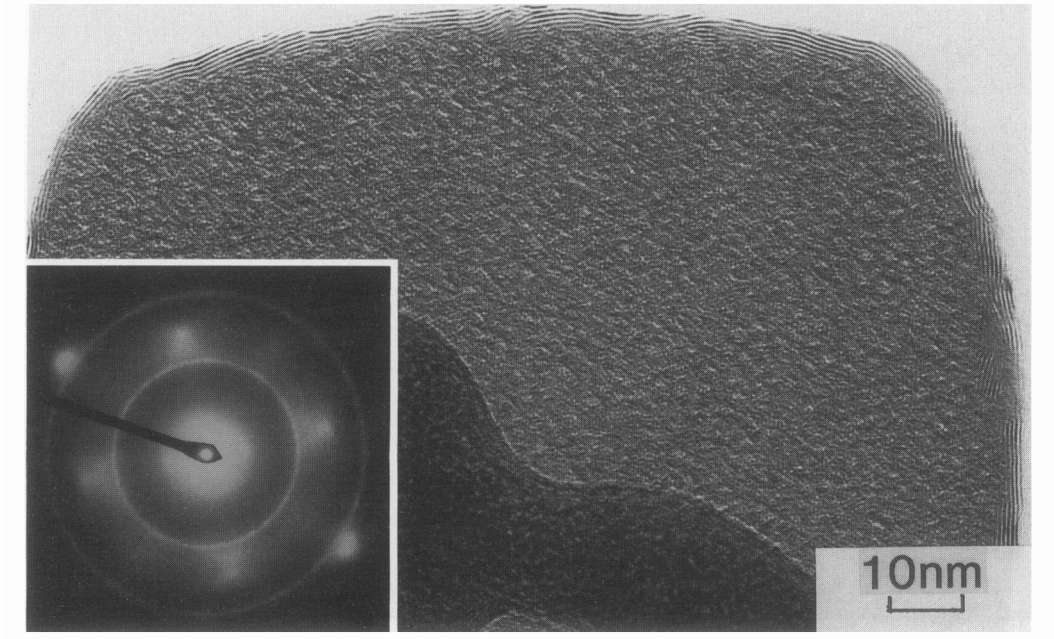

FIG. 4. Appearance in the TEM of a crystal of MoO_3 after sulfidation. It is now coated with a skin of MoS_2, about five sheets thick. The interior has a speckled appearance and its electron diffraction pattern (insert) shows this to consist of a highly disordered crystal of Mo metal. The rings in the pattern arise from the MoS_2. (Twenty percent MoO_3 on alumina.)

micrograph.) These appear as black lines when the sheets are roughly parallel to the electron beam. This hypothesis was tested by taking images at high magnification of the same area, tilted between exposures by about 5° increments. Examination of consecutive prints confirmed that those lines coming from plates of MoS_2 normal to the tilt axis were unchanged by the tilt, whereas those lying parallel to the tilt axis appeared and disappeared with tilt. No additional plates appeared with tilt. The behavior of selected flakes is illustrated in Fig. 5. This is the behavior to be expected for a planar sheet. According to our observations, the image of a single sheet seems to be visible for about ±5° of tilt. Now, as a result of the method of sample preparation and mounting, the flakes of alumina support material tend to orientate themselves dominantly parallel to the image plane of the microscope. The results of the tilt experiments and the fact that the image lines are usually straight are consistent with the hypothesis that the sheets are reasonably planar and stand roughly normal to the γ-Al_2O_3 surface. In some cases, there is evidence for alignment of the sheets such as might be expected if they were associated with surface steps (see Fig. 6). We can find no evidence for the presence of sheets of MoS_2 lying parallel to the surface of γ-Al_2O_3, but in general we do not see any MoS_2 at the edge of the γ-Al_2O_3, as is the case with other supports (vide infra).

It appeared that the size of the sheets increased with loading. These observations are summarized in Table 3. Because of the rough texture of the support, we were unable to determine whether or not the number of sheets increased with loading.

(*iii*) *Surface sulfide phase on zirconia.* For MoO_3 loadings greater than about 5%, the crystals of zirconia were generally coated

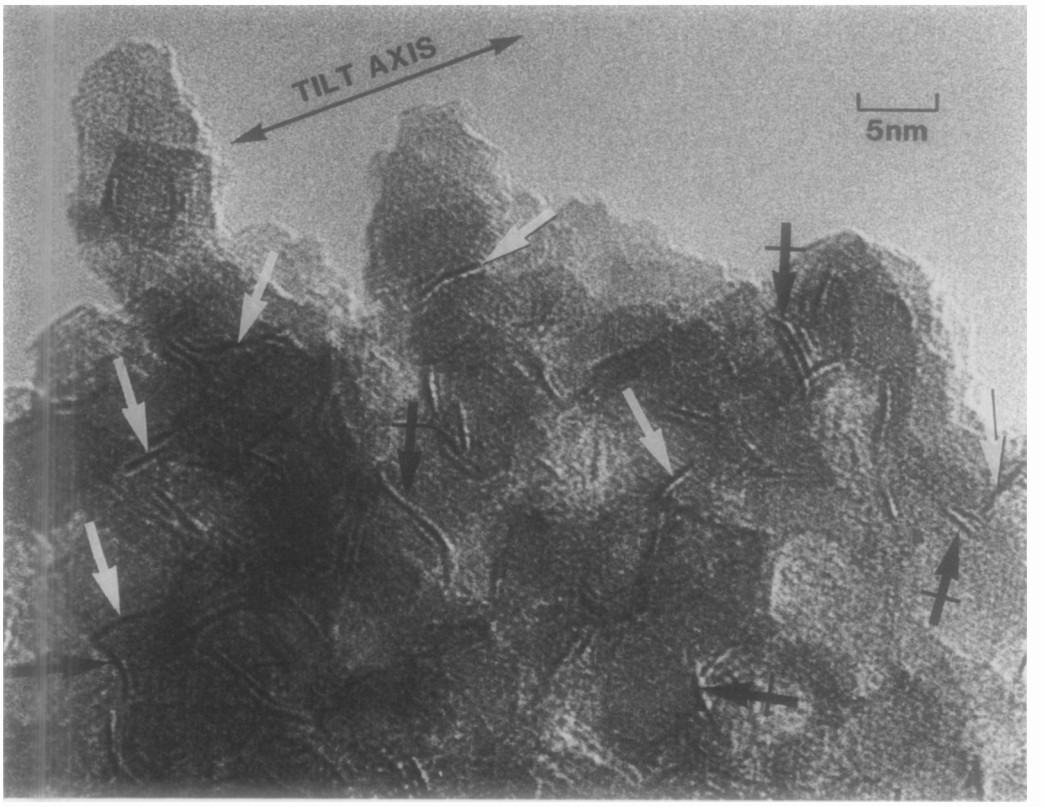

FIG. 5. Appearance in the TEM of MoS_2 (black lines) on γ-Al_2O_3 support. When the specimen is tilted about the axis shown, the black lines normal to the tilt axis (↕) remain visible over a range of ±20°. However, those parallel to the tilt axis (↑) appear and disappear as the specimen is tilted. (Ten percent MoO_3 on alumina.)

with a single sheet of MoS_2. At the appropriate focus condition of the TEM this appears in the micrographs as a single, intense black line surrounding each zirconia crystal (Fig. 7a). At low MoO_3 loadings this black line is discontinuous, implying that the zirconia crystals were only partly coated with the MoS_2 monolayer (Fig. 7b).

We suggest, therefore, that up to a specific value of MoO_3 surface concentration, all the Mo is adsorbed on the ZrO_2 and is subsequently sulfided to produce islands of an MoS_2 monolayer at low concentrations, while at higher concentrations a continuous monolayer of MoS_2 surrounds each zirconia crystal. When a complete monolayer is formed the surface exposed consists only of the sulfur atoms in the basal plane of the MoS_2 layer, and the original ZrO_2 surface is no longer exposed. Any excess Mo over monolayer requirements forms the sulfided

TABLE 3

Estimated Size of MoS_2 Sheets on Sulfided MoO_3/γ-Al_2O_3 Catalysts

% w/w MoO_3	Observations
5	mostly ≦3 nm
10	mostly ≦3 nm, some 5 nm
15	mostly 3–6 nm
30	mostly 3–6 nm, some 10 nm
40	mostly 6–10 nm

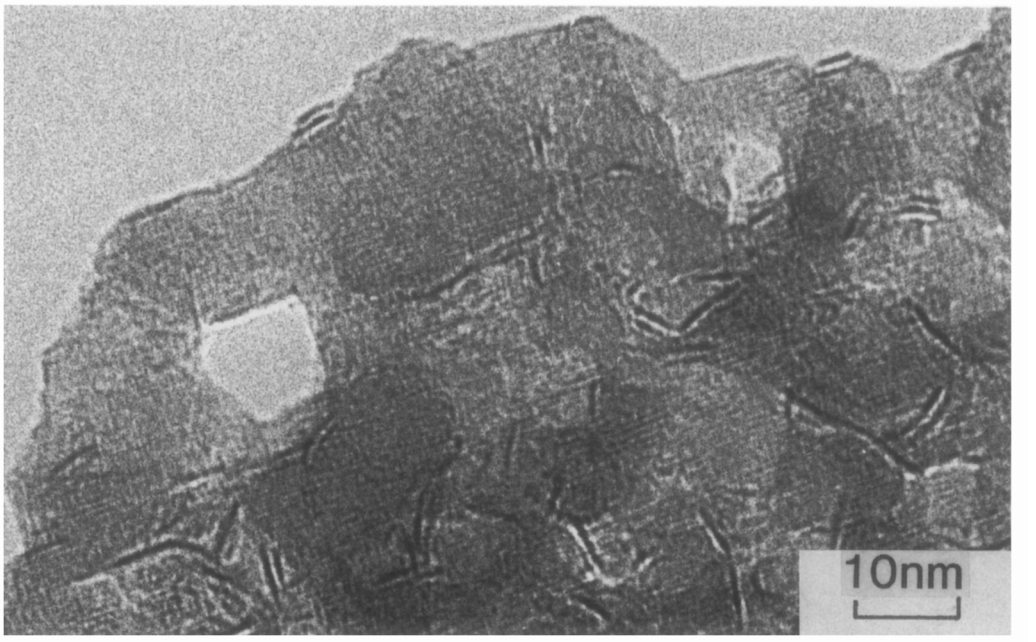

FIG. 6. Transmission electron micrograph of MoS_2 on a crystal of γ-Al_2O_3. In this case the MoS_2 sheets (black lines) are normal to the surface of the crystal and tend to be aligned with steps on the surface. (Ten percent MoO_3 on alumina.)

Mo crystals as a separate phase as already described.

(*iv*) *Surface sulfide phase on titania.* As was the case for zirconia, the titania becomes coated with a skin of MoS_2 lying parallel to the surface of the anatase crystals. However, in this case the layer is not restricted to a single monolayer but builds up in thickness with MoO_3 loadings greater than about 10%. Figure 8 shows a multilayer deposit of MoS_2 on TiO_2 as three to four black lines, with a spacing of about 0.6 nm around each anatase crystal. No excess MoS_2/Mo phase was found in these samples. There is some evidence of small amounts of excess MoS_2 as disordered patches of fringes, as indicated in Fig. 8 by arrows.

This material should therefore expose mainly the basal planes of MoS_2, with a constant exposed area for MoO_3 concentrations of more than about 5%. The original TiO_2 surface should no longer be exposed.

(*v*) *Surface sulfide phase on silica.* On silica, the MoS_2 takes the form of small "books," five to six layers thick and about 5–10 nm wide, dispersed over the surface, and standing generally normal to the surface. These books of MoS_2 appear in the TEM images as groups of fringes, each black line corresponding to an individual MoS_2 sheet (see Fig. 9). Unlike the sulfided Mo on ZrO_2 and TiO_2, at correct focus there is no black line around the edges of the SiO_2 particles.

DISCUSSION

The interpretation of the TEM images seems quite straightforward. By computer simulation of a through-focus series of images, we have demonstrated that a single sheet of MoS_2 (S-Mo-S) will give a single black line at a defocus of 50–60 nm for a tilt of about $\pm 5°$ to the electron beam (*22*). We expect that a single layer of MoS_2 on a crystal will generally behave in the same way

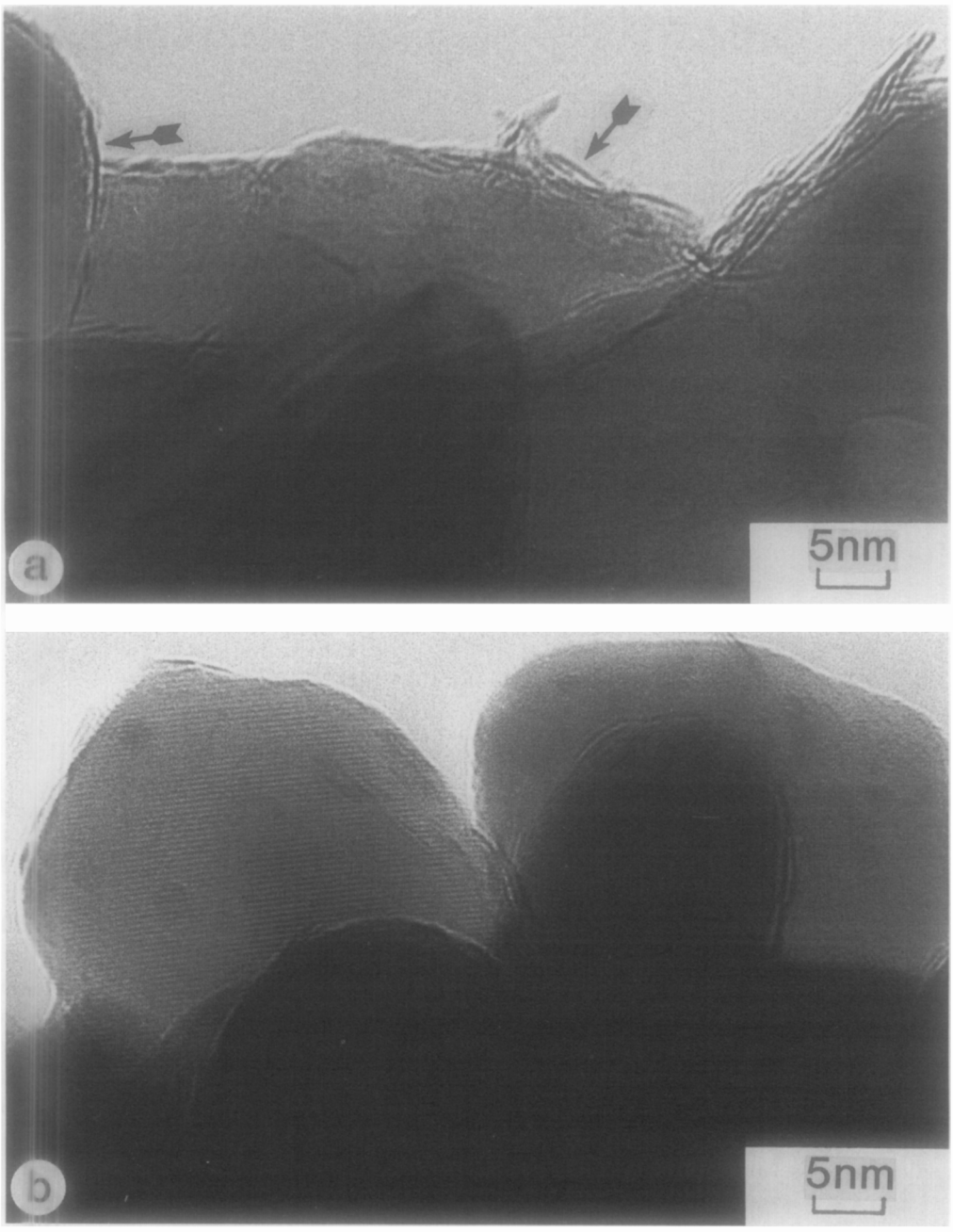

FIG. 7. Transmission electron micrographs of MoS_2 on ZrO_2. (a) With 6% MoO_3, the film is continuous and generally a monolayer (continuous single black line at the edge of the ZrO_2); (b) with smaller amounts, e.g., 1% MoO_3, the MoS_2 layer is discontinuous on the surface of the ZrO_2 crystals.

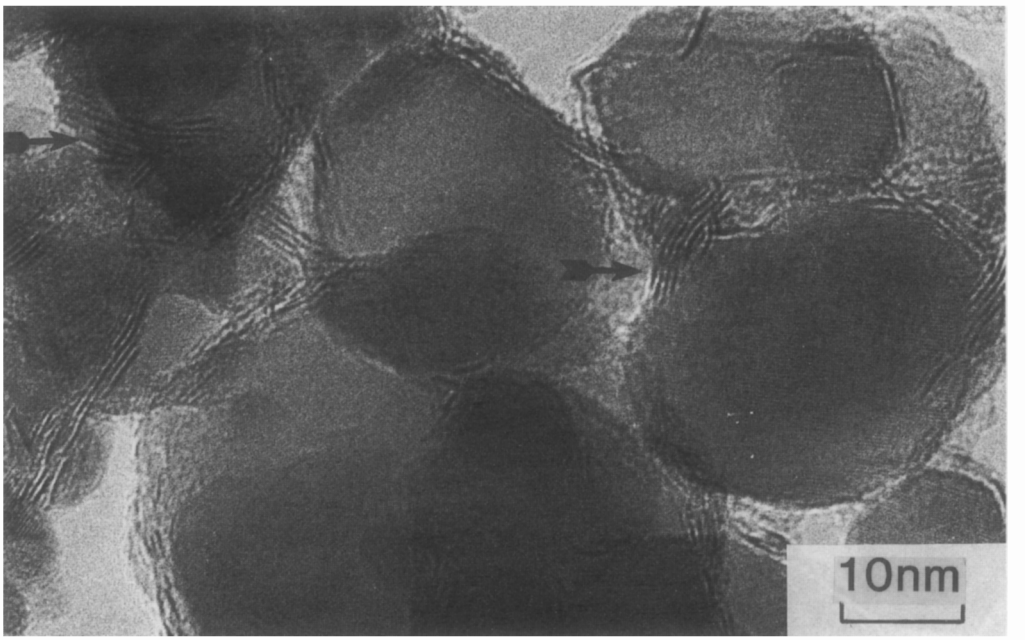

FIG. 8. Transmission electron micrographs of MoS_2 on TiO_2 showing a multilayer coating three to four layers around each crystal. Arrows show some evidence of small amounts of excess MoS_2 as disordered fringes.

and produce a strong black line at the edge of the crystal at the correct degree of underfocus. This should not be confused with Fresnel fringes which appear outside an edge at overfocus of the electron microscope.

Our observations of both bulk and surface oxide phases in the MoO_3/Al_2O_3 system are consistent with structural inferences made by spectroscopic methods (e.g., Refs. (*23–33*)). There is some variance of opinion in the literature as to whether the surface phase exists as one-dimensional chains (e.g., Ref. (*34*)), as a monolayer (*35, 36*), or as "patches" of monolayer and multilayer Mo (*32*). On the basis of EXAFS studies, Clausen *et al.* (*29*) conclude that in the calcined catalysts, molybdenum is present as isolated chains, ions, or small disordered patches rather than as well-defined compounds. Although our TEM studies can shed no direct light on this question, we are inclined to favor the existence of relatively isolated, disordered patches since clusters of 7–10 atoms should have been detectable under the conditions of the present TEM analysis.

For the surface sulfide phase our confirmation of the predominance of plates, one or more layers in thickness, standing perpendicularly to the support surface for alumina and silica is consistent with previous observations (*37, 38*). The existence of MoS_2 in this form implies a substantial morphological change in the process of transition from oxide to sulfide phase. Currently, there exists no understanding of the mechanism by which this occurs.

It is significant that the single layer "plates on edge" form of MoS_2 exists on the supports with the highest potential for interaction, i.e., the highest concentrations of surface hydroxyl groups. The tendency toward multilayer plates on the silica probably reflects the lower concentration of surface hydroxyl groups on silica compared to

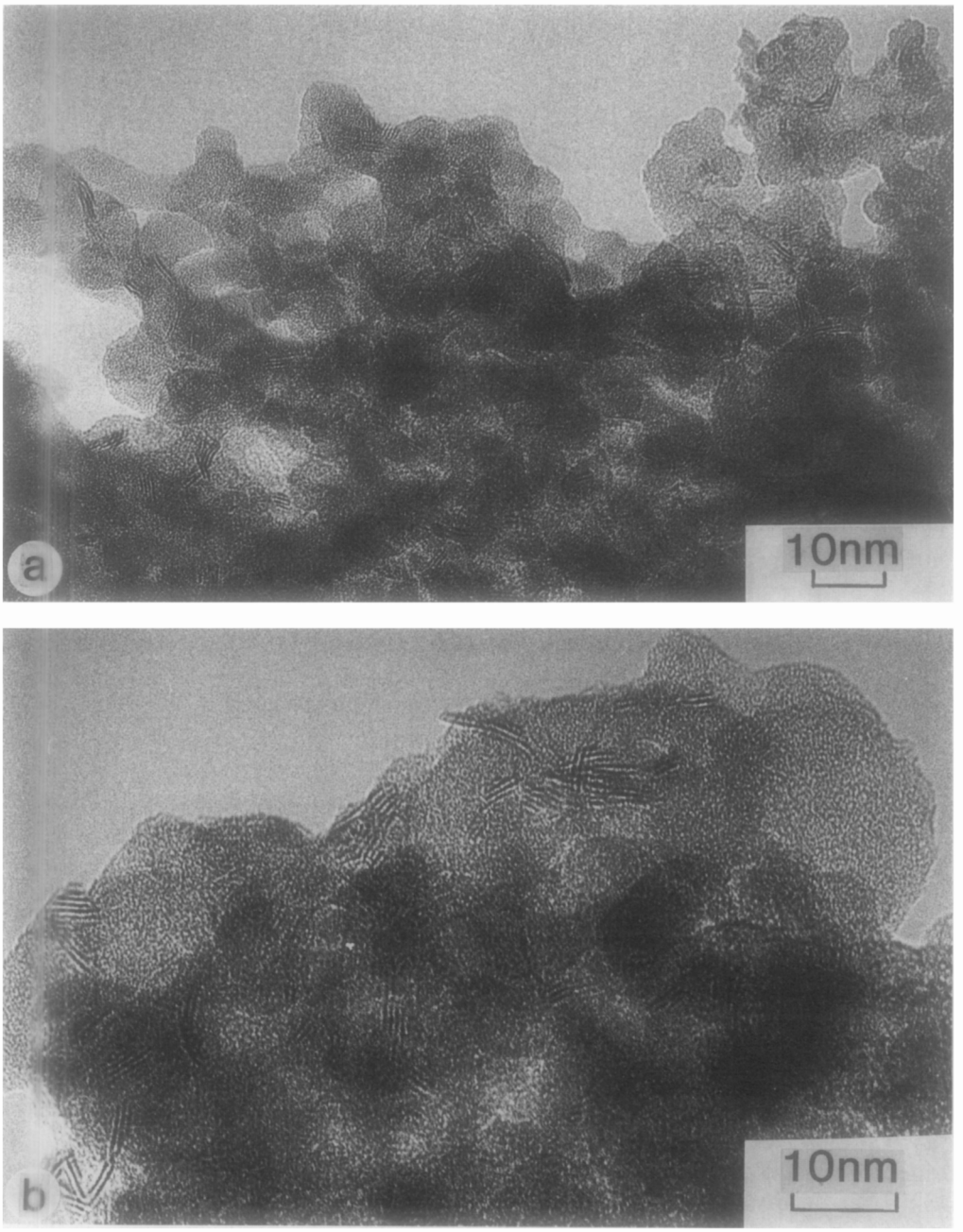

FIG. 9. Transmission electron micrographs of MoS_2 on SiO_2: (a) low magnification; (b) higher magnification. The MoS_2 forms "books" of up to five layers.

alumina, in that interlayer interactions (before and after sulfidation) will be more significant.

Our TEM observations of the morphology of the sulfided phases on ZrO_2 and TiO_2 are the first to be reported. Although we have previously observed the "skinning" phenomenon on unsupported Mo catalyst (*17, 18*), the eventual encapsulation of the support material was quite unexpected. The formation of expanding islands rather than detached plates presumably arises at least in part from the low concentration of surface hydroxyl groups on these supports. Multilayer formation of MoS_2 on the titania may reflect its very low bonding capability. Some considerable reactivity differences might be expected among the various supports, since after the formation of a complete monolayer of MoS_2 on ZrO_2 and TiO_2, the surface of the support is no longer available to the reactants. More importantly, as the islands expand to form the sulfide monolayer, the proportion of edge Mo atoms finally decreases to zero. At this point, only the basal plane of the MoS_2 is available to the reactants.

Unlike the surface phases, the morphology of the bulk oxide phases is retained after sulfiding. Again the phenomenon of skin formation occurs. The MoO_3 becomes skinned with 5–10 layers of MoS_2 over a core of disordered Mo metal. Metallic molybdenum in reduced or sulfided catalysts has been indicated in several studies (*39–41*), and the present work shows that it is located within the sulfide species originating from bulk MoO_3. On alumina, the tubular structures ascribed to $Al_2(MoO_4)_3$ are also skinned with MoS_2, over a disordered core material which we were not able to identify. It appears likely that the layers of MoS_2 "passivate" the surface of the bulk oxides, preventing diffusion of H_2S for further sulfidation. Hydrogen then diffuses through the surface layers and reduces the core. As these bulk species have a low specific surface area and consist entirely of basal planes, we may conclude that they make

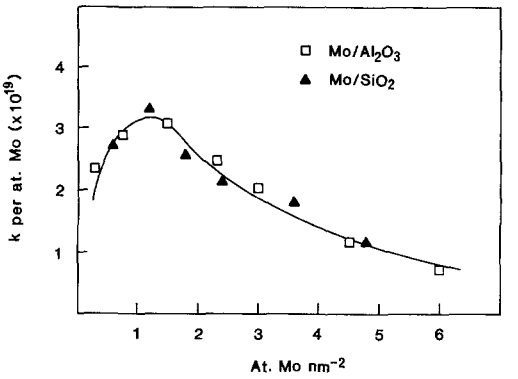

FIG. 10. The specific activity (per molybdenum atom) for the hydrodesulfurization of thiophene at 648 K of molybdenum sulfide catalysts supported on Al_2O_3 and SiO_2 versus surface concentration of Mo (atoms per square nanometer of support).

no significant contribution to the catalytic activity. Indeed, it has been shown that these bulk species may be dissolved out of the catalyst by an ammonia solution, with no apparent loss of activity (*23, 42*).

The reactivity data may now be examined in the light of TEM results. The disparity in surface areas of the various supports makes comparison on the basis of Table 1 difficult. In Figs. 10 and 11 the data are replotted to allow comparison of an activity per molybdenum atom as a function of surface concentration (atoms of molybdenum per square nanometer of support). The shape of the curves in Figs. 10 and 11 is characteristic of the observed morphology of MoS_2.

For the silica and alumina supports, both sets of data now lie on the one curve, which displays a maximum in specific activity at a surface concentration of about 1.5 atoms of molybdenum per square nanometer (corresponding to 10% w/w of MoO_3 on the alumina and around 12.5% w/w MoO_3 on the silica). Other data in the literature for thiophene HDS over MoO_3 on alumina catalysts show a similar maximum in specific activity at around 1.5 Mo atoms per square nanometer (*19, 43, 44*). This concentration is well below the theoretical monolayer coverage of around six atoms of Mo per square nano-

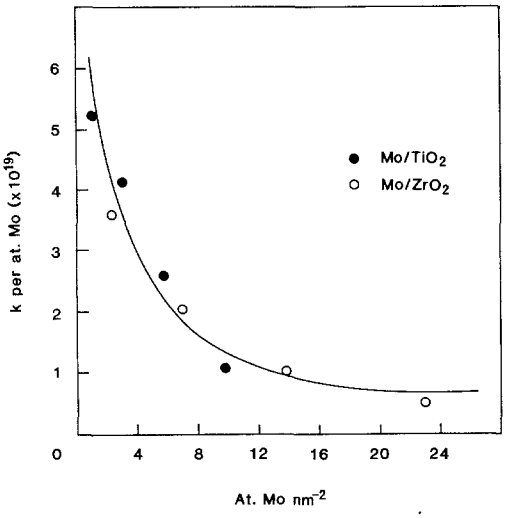

FIG. 11. The specific activity (per molybdenum atom) for the hydrodesulfurization of thiophene at 648 K of molybdenum sulfide catalysts supported on TiO_2 and ZrO_2 versus surface concentration of Mo (atoms per square nanometer of support).

meter (*45*). The results of our work do not impute any particular significance to this concentration.

For the systems which resulted in "island" morphology (TiO_2 and ZrO_2) we observed a monotonic decrease in specific activity with surface concentration. (Note, however, the expanded range of loadings compared to the SiO_2/Al_2O_3 systems: it is possible that a maximum may exist in the range 1–2 at. Mo nm^{-2} which was not examined in detail, owing to the very low activity of these catalysts.) It seems likely that differences in the activity patterns for the two groups of catalysts have their origins in the morphological differences. For example, adsorption of thiophene at an edge site of MoS_2 lying flat on the support may be sterically hindered. Adsorption at edge sites on flakes of MoS_2 attached vertically to the support would not be hindered. Further, the possibility of extensive support interaction (by analogy with SMSI) would be greater for a flake of MoS_2 lying flat on the support. In this connection, we have recently observed that the ESR spectral behaviors of MoS_2 on titania and zirconia are similar, but differ from that of alumina (*46*). Indications of significant Mo–support interactions in both oxide and sulfide catalysts have appeared in ESCA studies (*14, 47*). We suggest therefore that the different activity patterns observed for the different supports are the result of flakes of MoS_2 standing dominantly vertically on Al_2O_3 and SiO_2, but lying flat on the support in the case of ZrO_2 and TiO_2.

The final observation which may be made upon the kinetic results is that the specific activity of Mo at low surface concentration on titania and zirconia is significantly higher than that for alumina or silica. Therefore, if sufficient Mo could be dispersed at low surface coverage on titania or zirconia, then a more active catalyst would result. This effectively requires a high-surface-area titania or zirconia support. However, there are difficulties in obtaining titania or zirconia with a thermally stable high surface area.

Thus, the activity behavior of the different catalysts corresponds broadly with the observed differences in morphology. The reasons for the occurrence of such diverse morphologies are not at present understood. In the first instance we believe that the oxidic phase is deposited in patches on the surface of the supports, presumably attached via OH groups. Alumina will possess the greatest density of hydroxyl groups, followed by silica and then zirconia and titania (*48*).

Spectroscopic studies of reduction and sulfiding (*21, 49–54*) have shown that breaking of Mo-O-Al linkages can occur, leading to detachment and subsequent sulfiding of the oxide patches with repopulation of the support surface by OH and possibly SH groups. Thus the two-dimensional slabs of MoS_2 are created. The process whereby these slabs adopt a vertical position on alumina and silica is not clear and requires further investigation.

Certainly, the high energy edge planes possess greater reactivity than the basal planes and thus edge-bonding via a "hinge species," perhaps involving the strongest

OH bonds, could lead to the vertical configuration.

Additionally, Hayden and Dumesic (*37*) have drawn attention to the favorable spacing relationships existing between Mo-Mo in the $(2\bar{1}10)$ plane of MoS_2 and the O–O in the (110) plane of alumina that could lead to slabs of MoS_2 stacked perpendicularly to the alumina surface. Similar observations have been made for edge-bonding of WS_2 via the $(2\bar{1}10)$ plane to silica (*55, 56*). Hayden and Dumesic (*37*) and Topsøe and Topsøe (*53*) have shown that high-temperature sulfiding can destroy these hinge species and produce flakes lying parallel to the surface of alumina.

The factors responsible for the different morphologies of MoS_2 occurring on titania and zirconia are not clear. It may be that characteristic lattice parameters of the support surfaces favor epitaxial growth of MoS_2 rather than edge bonding. The higher specific activity of MoS_2 on ZrO_2 and TiO_2, however, suggests the possibility of a significant interaction between the sulfide phase and the surface. This interaction might be with metal atoms directly, through oxo links, or with OH or SH groups underlying or surrounding the "islands" or "rafts."

CONCLUSIONS

This study has demonstrated that the dominant morphology of MoS_2 surface species supported on alumina or silica is in the form of flakes of "MoS_2" containing from one to six layers, located vertically to the surface of the support. By contrast, when molybdenum is supported on titania (anatase) or zirconia, the MoS_2 surface species consists of "raftlike" structures, sitting flat on the support. At higher loadings, the rafts expand to coat the support in a continuous layer, thus exposing only the basal planes of the MoS_2. On all the supports except titania, a bulk sulfide phase derived from bulk MoO_3 exists at higher loadings. This material consists of a surface skin of MoS_2, up to 10 layers thick, surrounding a core of molybdenum metal. Thus, the metallic molybdenum detected in earlier ESCA studies is located within one of the bulk phases existing on the support. On alumina, a second bulk phase exists. In the oxidic form, it displayed a tubular appearance, and electron diffraction showed it to be $Al_2(MoO_4)_3$. In the sulfided form, the tubular morphology was retained, and again multiple layers of MoS_2 formed a skin over a core of an unidentified material. While our results do not preclude the formation of a "surface" aluminium molybdate, we have demonstrated that this material may exist as a separate bulk phase. Activity data for the hydrodesulfurization of thiophene displayed two different types of characteristics according to the morphology of the surface MoS_2. The specific activity of molybdenum on titania and zirconia at lower surface concentrations was much higher than that for alumina- or silica-supported catalysts, suggesting a significant support interaction.

The fact that distinctly different forms of MoS_2 can be created at the same surface loading and employing the same preparation procedures will prove extremely valuable in the study of these materials. The means by which molybdenum species change from patches of monolayer to vertically oriented plates of MoS_2 on alumina and silica is currently unresolved and deserves some attention. Studies are underway in this laboratory which are aimed at defining this process and at determining the influence of promoters on the morphology of the bulk and surface phases of supported molybdenum sulfide catalysts.

REFERENCES

1. Gates, B. C., Katzer, J. B., and Schuit, G. C. A., "Chemistry of Catalytic Processes," McGraw–Hill, New York, 1979.
2. Farragher, A. L., and Cossee, P., *in* "Proceedings, 5th International Congress on Catalysis, Palm Beach, 1972" (J. W. Hightower, Ed.), p. 1301. North-Holland, Amsterdam, 1973.
3. Delmon, B., *in* "Proceedings of the Third International Conference on Chemistry and Uses of Mo-

lybdenum" (H. F. Barry and P. C. H. Mitchell, Eds.), p 73. Climax Molybdenum Co. Ann Arbor, MI, 1979.
4. Delmon, B., *React. Kinet. Catal. Lett.* **13,** 203 (1980).
5. Pirotte, D., Zabala, J. M., Grange, P., and Delmon, B., *Bull. Soc. Chim. Belg.* **90,** 1239 (1981).
6. Topsøe, H., Candia, R., Topsøe, N-Y., and Clausen, B. S., *Bull. Soc. Chim. Belg.* **93,** 783 (1984).
7. Topsøe, H., Clausen, B. S., Topsøe, N-Y., and Pedersen, E., *Ind. Eng. Chem. Fund.* **25,** 25 (1986).
8. Topsøe, H., Topsøe, N-Y, Sørensen, O., Candia, R., Clausen, B. S., Kallesoe, S., and Pedersen, E., *Prepr. Amer. Chem. Soc. Div. Pet.Chem.* **28,** 1252 (1983).
9. Sørensen, O., Clausen, B. S., Candia, R., and Topsøe, H., *Appl. Catal.* **13,** 363 (1985).
10. Pollack, S. S., Sanders, J. J., and Fischer, R. E., *Appl. Catal.* **8,** 383 (1983).
11. Topsøe, H., *in* "Surface Properties and Catalysis by Non-metals: Oxides, Sulfides, and Other Transition Metal Compounds" (J. P. Bonnelle, B. Delmon, and E. G. Derouane, Eds.), p. 329. Reidel, Dordrecht, 1983.
12. Muralidhar, G., Massoth, F. E., and Shabtai, J., *J. Catal.* **85,** 44 (1984).
13. Nishijima, A., Shimada, H., Sato, T., Yoshimura, Y., and Hiraishi, J., *Polyhedron* **5,** 243 (1986).
14. Shimade, H., Sato, T., Yoshimura, Y., Hiraishi, J., and Nishijima, A., *J. Catal.* **110,** 275 (1988).
15. Breysse, M., Bennett, B. A., Chadwick, D., and Vrinat, M., *Bull. Soc. Chim. Belg.* **90,** 1271 (1981).
16. de Beer, V. H. J., Duchet, J. C., and Prins, R., *J. Catal.* **72,** 369 (1981).
17. Pratt, K. C., Sanders, J. V., and Tamp, N., *J. Catal.* **66,** 82 (1980).
18. Sanders, J. V., and Pratt, K. C., *J. Catal.* **67,** 331 (1981).
19. de Beer, V. H. J., van der Aalst, M. J. M., Machiels, C. J., and Schuit, G. C. A., *J. Catal.* **43,** 78 (1976).
20. Leyrer, J., Vielhaber, B., Zaki, M. I., Zhuang, S., Weitkamp, J., and Knözinger, H., *Mater. Chem. Phys.* **13,** 301 (1985).
21. Delannay, F., *Appl. Catal.* **16,** (1985).
22. Sanders, J. V., and Lynch, D. F., unpublished results.
23. Giordano, N., Bart, J. C. J., Vaghi, A., Castellan, A., and Martinotti, G., *J. Catal.* **36,** 81 (1975).
24. Jeziorowski, H., and Knözinger, H., *J. Phys. Chem.* **83,** 1166 (1979).
25. Cheng, C. P., and Schrader, G. L., *J. Catal.* **60,** 276 (1979).
26. Zingg, D. S., Makovsky, L. E., Tischer, R. E., Brown, F. R., and Hercules, D. M., *J. Phys. Chem.* **84,** 2898 (1980).
27. Grange, P., *Catal. Rev.-Sci. Eng.* **21,** 135 (1980).
28. Ratnasamy, P., and Sivasanker, S., *Catal. Rev. Sci. Eng.* **22,** 401 (1980).
29. Clausen, B. S., Topsøe, H., Candia, R., Villadsen, J., Lengeler, B., Als-Nielsen, J., and Christensen, F., *J. Phys. Chem.* **85,** 3868 (1981).
30. Yao, H. C., *J. Catal.* **70,** 440 (1981).
31. Thomas, R., van Oers, E. M., de Beer, V. H. J., Medema, J., and Moulijn, J. A., *J. Catal.* **76,** 241 (1982).
32. Wang, L., and Hall, W. K., *J. Catal.* **83,** 242 (1983).
33. Massoth, F. E., Muralidhar, G., and Shabtai, J., *J. Catal.* **85,** 53 (1984).
34. Weigold, H., *J. Catal.* **83,** 85 (1983).
35. Massoth, F. E., *in* "Advances in Catalysis" (D. D. Eley, H. Pines, and P. B. Weisz, Eds.), Vol. 27, p. 265. Academic Press, San Diego, 1978.
36. Schuit, G. C. A., and Gates, B. C., *AIChE J.* **19,** 417 (1973).
37. Hayden, T. F., and Dumesic, J. A., *J. Catal.* **103,** 366 (1987).
38. Zaikovskii, V. I., Plyasova, L. M., Burmistrov, V. A., Startsev, A. N., and Yermakov, Y. I., *Appl. Catal.* **11,** 15 (1984).
39. Murchison, C. B., *in* "Proceedings, 4th Int. Conf. on Chemistry and Uses of Molybdenum, Golden, Colorado, 1982" (H. F. Barry and P. C. H. Mitchell, Eds.), p. 197. Climax Molybdenum Co., Ann Arbor, 1982.
40. Muralidhar, G., Concha, B. E., Bartholomew, G., and Bartholomew, C. H., *J. Catal.* **89,** 274 (1984).
41. Concha, B. E., Bartholomew, G. L., and Bartholomew, C. H., *J. Catal.* **89,** 536 (1984).
42. Kotera, K., Todo, N., Muramatsu, K., Ogawa, K., Kurita, M., Sato, T., Ogawa, M., and Kabe, T., *Int. Chem. Eng.* **11,** 752 (1971).
43. Bachelier, J., Tilliette, M. J., Duchet, J. C., and Cornet, D., *J. Catal.* **76,** 300 (1982).
44. Okamoto, Y., Tomioka, H., Imanaka, T., and Teranishi, S., *J. Catal.* **66,** 93 (1980).
45. Sonnemans, J., and Mars, P., *J. Catal.* **31,** 209 (1973).
46. Oliver, S. W., Smith, T. D., Pilbrow, J. R., Pratt, K. C., and Christov, V., *J. Catal.* **111,** 88 (1988).
47. Nag, N. K., *J. Phys. Chem.* **91,** 2324 (1987).
48. Muralidhar, G., Massoth, F. E., and Shabtai, J., *Prepr. Amer. Chem. Soc. Div. Pet. Chem.* **27**(3), 722 (1982).
49. Millman, W. S., Crespin, M., Cirillo, A. C., Abdo, S., and Hall, W. K., *J. Catal.* **60,** 404 (1979).
50. Houalla, M., Kibby, C. L., Petrakis, L., and Hercules, D. M., *J. Catal.* **83,** 50 (1983).
51. Topsøe, N-Y., *J. Catal.* **64,** 235 (1980).
52. Maternova, J., *Appl. Catal.* **6,** 61 (1983).

53. Topsøe, N-Y., and Topsøe, H., *Bull. Soc. Chim. Belg.* **90,** 1311 (1981).
54. Seyedmonir, S. R., Abdo, S., and Howe, R. F., *J. Phys. Chem.* **86,** 1233 (1982).
55. Moroz, E. M., Bogdanov, S. V., Tsybulya, S. V., Burmistrov, V. A., Stratsev, A. N., and Yermakov, Y. I., *Appl. Catal.* **11,** 173 (1984).
56. Yermakov, Y. I., Startsev, A. N., Burmistrov, V. A., Shumilo, O. N., and Bulgakov, N. N., *Appl. Catal.* **18,** 33 (1985).